VII International Conference on Particle-Based Methods
PARTICLES 2021
P. Wriggers, M. Bischoff, E. Oñate, M. Bischoff, A. Düster & T. Zohdi (Eds)

A DEM GENERALIZED KELVIN CONTACT MODEL FOR PREDICTING STIFFNESS OF ASPHALT MIXTURES

GUSTAVO CÂMARA[1], NUNO AZEVEDO[2] AND RUI MICAELO[3]

[1] DEC, NOVA School of Science and Technology (FCT - NOVA)
Caparica, Portugal
e-mail: g.camara@campus.fct.unl.pt

[2] Portuguese National Laboratory for Civil Engineering (LNEC)
Avenida do Brasil, 101, Lisbon, Portugal
email: nazevedo@lnec.pt

[3] CERIS, DEC, NOVA School of Science and Technology (FCT - NOVA)
Caparica, Portugal
email: ruilbm@fct.unl.pt

Key words: Asphalt mastic, Viscoelastic, Particle model, Generalized Kelvin

Abstract. This paper presents the development of a three-dimensional micromechanical model based on the Laguerre-Voronoi diagrams of the grain structure to study the viscoelastic behaviour of asphalt mastic with the use of the discrete element method (DEM). Usually, the DEM models of asphalt mastics adopt a Burger's contact model to reproduce the known viscoelastic behaviour. A generalized Kelvin chain model (GK) was developed within a particle model (PM) framework in order to obtain a better agreement in the determination of dynamic properties of mastics. Numerical cyclic tests under a frequency range varying from 10 to 0.10 Hz were implemented to analyse the dynamic response. The parameters of the DEM model are determined from macroscale material properties, which are obtained by fitting lab-based dynamic modulus and phase angle results. The influence of the parameters defining the contact models on the dynamic response was investigated. An iterative procedure was derived to convert the macroscale properties into calibrated contact parameters of the proposed model. Simulation tests show a good correlation between the numerical results obtained with the GK contact model and the experimental data when compared with the agreement obtained with the Burger's model.

1 INTRODUCTION

Asphalt mixture is a composite material usually comprising coarse and fine aggregates, air voids and bitumen. The mix between the fine aggregates and the bitumen is called mastic, which is considered the real binder of the asphalt pavements. The behaviour of the asphalt mixtures is governed by the interaction of their different constituent elements. The mastic provides the time and temperature dependency and influences the general behaviour of important properties, such as the dynamic modulus, cohesion and relaxation characteristics of the asphalt mixtures.

In order to reduce costly tests for the design and control of the asphalt pavements, the behaviour of the mixtures have been studied by researchers over the years following a micromechanical approach based on their individual components. One of these techniques is the discrete element modelling (DEM) [1]. The DEM is a numerical model based on the alternate application of the Newton's Second Law (the law of motion) and the force-displacement law, applied to the particles and contacts, respectively [2]. A time stepping procedure is used to integrate the constitutive equations for each entity of the particle assembly.

The use of micromechanical approaches based on the DEM has been widely used to investigate the properties of asphalt mixtures and mastics over the past years. Besides, this methodology has the advantages of considering the material structure, the constitutive laws are based on force-displacement relationships and the possibility to measure large displacements and crack propagation [3]. A brief summary of some study efforts is provided in the following section.

2 DISCRETE ELEMENT MODELLING BACKGROUND

The DEM was first introduced by Cundall [2, 4] in the analysis of rock mechanics. In the asphalt materials field, the first study with the use of the discrete element modelling approach was presented in [5]. The authors were able to prove possible the numerical simulation in the analysis of a two-dimensional asphalt structure, modelling the aggregate-binder and the inter-granular interactions in the presence of bitumen with elastic aggregates using a viscoelastic contact model.

Few years later, a micromechanical model for hot mix asphalt was proposed in [6]. In this analysis, the Burger's contact model was applied to represent viscoelastic behaviour of the binder in the asphalt-aggregate contact. It was shown that the stress-strain response was correctly simulated. In many of the efforts in the study of asphalt materials, elastic models were assumed to simulate the contact behaviour of the mastic [7, 8]. As a consequence, the time-dependent behaviour of this material was difficult to be measured.

In order to compute the viscoelasticity of such materials, many studies have been focused on the implementation of viscoelastic contact models. In most of the analysis, the Burger's contact model has been implemented to simulate the interactions among the contacting particles of the mastic. By simulating cyclic tests for predicting the dynamic modulus and phase angle of asphalt mastics, Liu *et al.* [9] determined the behaviour of these materials under a loading frequency range. Using the Burger's model to represent the viscoelasticity of the mastic, the dynamic response was accurately predicted compared to lab tests, with a confidence rate of more than 90%. A similar work was developed in [10], where a maximum error between the dynamic behaviours in discrete model predictions and lab-based data was less than 10%. A considerable reduction in the computational time in DEM analysis based on the frequency-temperature superposition principle was achieved in [11]. Similar to other studies, the authors adopted the Burger's model to investigate the dynamic behaviour at different temperatures and loading frequencies of asphalt materials.

However, the Burger's contact model is not suitable for predicting the viscoelastic behaviour of asphalt mixtures and mastics along a large frequency range. The errors between the DEM analysis and experimental results in dynamic tests may decrease with the implementation of more complex contact models, such as the generalized Maxwell model and the generalized Kelvin model [11]. In [12], a generalized Maxwell model was used to simulate the time-dependent behaviour of mastics at low-temperatures in dynamic modulus tests, static creep tests and bending tests. The results showed a maximum error of 8% between numerical and lab measurements among the different analysis.

By the same reason, this work describes a new approach in the analysis of the viscous behaviour of mastic in the context of DEM. In order of that, a generalized Kelvin contact model is derived and a calibration method of the contact parameters is presented based on values of dynamic modulus and phase angle experimentally obtained for a variety of loading frequencies. The method is based on a direct integration of the constitutive equations, using a centred difference scheme, similar to the adopted in [13] for the Burger's model equations.

3 OBJECTIVES AND SCOPE

The main objective of this paper is to develop a generalized Kelvin contact model with the use of the discrete element method to characterize the viscoelastic behaviour of asphalt mastics across a loading frequency range. The proposed contact model is derived, as so as the model implementation and the calculation process to obtain the contact parameters. The contact parameters are obtained from macroscale parameters fitting experimental data. Macroscopic parameters are properties defining the mechanical behaviour of bituminous mastic. The procedure to convert the macroscale properties into microscale parameters, i.e. contact parameters, is established. For last, the proposed model is calibrated using compressive cyclic tests at different loading frequencies submitted to a strain control mechanism. The response obtained with the proposed model is compared to the results obtained with the traditional Burger's contact model.

4 DISCRETE ELEMENT VISCOELASTIC CONTACT MODEL

A generalized Kelvin model was developed to represent the time-dependency of mastic samples. This model consists of a Maxwell model element (a spring and a dashpot are connected in series) and n-chains of Kelvin elements (springs and dashpots are connected in parallel) placed in series, as illustrated in Figure 1.

The generalized Kelvin model (GK) adopts a direct integration of the constitutive equations, using a centred difference scheme, similar to the adopted in [13] for the Burger's model equations. The total displacement (u) of the contact model results from the sum of the elastic deformation of the spring (u_κ) and the irreversible deformation of the dashpot unit (u_η) of the Maxwell element, respectively, which correspond to the Maxwell element's total displacement, and the sum of the delayed elastic deformation from the ith Kelvin element (u_i), as shown in equation 1. On the other hand, the generalized Kelvin vis-

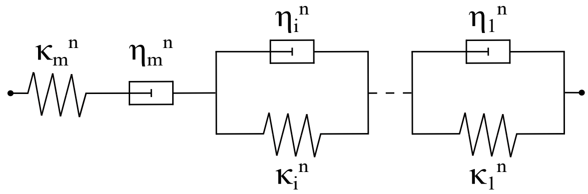

Figure 1: Generalized Kelvin contact model

coelastic contact model's force (f) and the forces generated by these elements (f_κ, f_η and f_i) are the same, as stated in equation 2.

$$u = \sum_{i=1}^{m} u_i + u_\kappa + u_\eta \tag{1}$$

$$f = f_i = f_\kappa = f_\eta \tag{2}$$

The force-displacement relationship of the ith Kelvin element and the Maxwell element are expressed in equations 3-5.

$$\dot{u}_i = \frac{f}{\eta_i} - \frac{\kappa_i u_i}{\eta_i} \tag{3}$$

$$\dot{u}_\kappa = \frac{\dot{f}}{\kappa_m} \tag{4}$$

$$\dot{u}_\eta = \frac{f}{\eta_m} \tag{5}$$

Taking the equation 3 and applying the central difference approximation and average values for the derivative units and solving the equation for the derivative unit of the Kelvin's displacement chain versus time, equation 3 can be expressed as:

$$\frac{u_i^{t+1} - u_i^t}{\Delta t} = \frac{1}{\eta_i}\left[\frac{f^{t+1} + f^t}{2} - \kappa_i \frac{u_i^{t+1} + u_i^t}{2}\right] \tag{6}$$

where Δt is the adopted time step.

By solving the equation 6 to the delayed displacement of the Kelvin contact model at time $t+1$, it is determined the displacement of the ith element of the Kelvin parcel.

$$u_i^{t+1} = \frac{1}{A_i}\left[B_i u_i^t + \frac{\Delta t}{2\eta_i}\left(f^{t+1} + f^t\right)\right] \tag{7}$$

where the values of parameters A_i and B_i are determined according to the following equations:

$$A_i = 1 + \frac{\kappa_i \Delta t}{2\eta_i} \tag{8}$$

$$B_i = 1 - \frac{\kappa_i \Delta t}{2\eta_i} \tag{9}$$

The first derivative of the total displacement of the Maxwell unit (u_m) is determined by the sum of equations 4 and 5.

$$\dot{u}_m = \frac{\dot{f}}{\kappa_m} + \frac{f}{\eta_m} \tag{10}$$

Applying the central difference approximation and average values, the displacement of the spring and dashpot units of the Maxwell element at time $t+1$ is expressed as:

$$u_m^{t+1} = \frac{f^{t+1} - f^t}{\kappa_m} + \frac{\Delta t\,(f^{t+1} + f^t)}{2\eta_m} + u_m^t \tag{11}$$

Substituting the equations 7 and 11 into the first derivative of equation 1, the normal and shear force-displacement relationships of the generalized Kelvin contact model is expressed according to equation 12.

$$f^{t+1} = \frac{1}{C}\left[u^{t+1} - u^t + \left(1 - \sum_{i=1}^{m} \frac{B_i}{A_i}\right) u_i^t - Df^t\right] \tag{12}$$

where C and D are determined according to equations 13 and 14, respectively.

$$C = \sum_{i=1}^{m} \left(\frac{\Delta t}{2A_i\eta_i}\right) + \frac{1}{\kappa_m} + \frac{\Delta t}{2\eta_m} \tag{13}$$

$$D = \sum_{i=1}^{m} \left(\frac{\Delta t}{2A_i\eta_i}\right) - \frac{1}{\kappa_m} + \frac{\Delta t}{2\eta_m} \tag{14}$$

5 MACROSCOPIC PARAMETERS OF THE GENERALIZED KELVIN MODEL

In this research, a macroscopic generalized Kelvin viscoelastic model was employed to fit the laboratory data of dynamic modulus and phase angle of asphalt mastic. The macroscopic model and its parameters are represented in Figure 2.

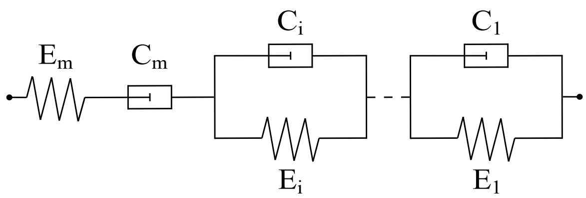

Figure 2: Macroscopic generalized Kelvin model

Taking the force-displacement relationship in equations 1 to 5 as reference, the stress and strain relationships are expressed according to equations 15-17.

$$\varepsilon_{Em} + \varepsilon_{Cm} + \sum_{i=1}^{m} \varepsilon_i \tag{15}$$

$$\sigma = \sigma_{Em} = \sigma_{Cm} = \sigma_E^i \tag{16}$$

$$\sigma_{Em} = E_m \varepsilon_{Em} \qquad \sigma_{Cm} = C_m \varepsilon_{Cm} \qquad \sigma_E^i = E_i \varepsilon_i + C_i \varepsilon_i \tag{17}$$

The sinusoidal one-dimensional loading applied to the model and the resultant strain are determined according to equations 18 and 19, respectively.

$$\sigma(t) = \sigma_0 e^{i\omega t} \tag{18}$$

$$\varepsilon(t) = \varepsilon_0 e^{i(\omega t - \phi)} \tag{19}$$

where σ_0 and ε_0 refer to the stress and strain amplitudes, ω is the angular frequency and ϕ is the phase angle.

Substituting the equations 18 and 19 into equation 17 results in the following expressions:

$$\sigma_0 e^{i\omega t} = E_m \varepsilon_{Em} e^{i(\omega t - \phi)} \tag{20}$$

$$\sigma_0 e^{i\omega t} = i\omega C_m \varepsilon_{Cm} e^{i(\omega t - \phi)} \tag{21}$$

$$\sigma_0 e^{i\omega t} = E_i \varepsilon_i e^{i(\omega t - \phi)} + i\omega C_i \varepsilon_i e^{i(\omega t - \phi)} \tag{22}$$

The complex modulus (E^*) is determined by the ratio between the applied stress (equation 18) and the resultant strain (equation 19), as expressed in equation 23. It is composed by a real part ($E^{'}$), which corresponds to the storage modulus, and an imaginary part ($E^{''}$), corresponding to the loss modulus in a loading cycle.

$$E^* = \frac{\sigma_0 e^{i\omega t}}{\varepsilon_0 e^{i(\omega t - \phi)}} = \frac{\sigma_0}{\varepsilon_0} e^{i\phi} \tag{23}$$

The strains of the elements of the model can be obtained by solving the equations 24-26.

$$\varepsilon_{Em} = \frac{\sigma_0 e^{i\omega t}}{E_m e^{i(\omega t - \phi)}} = \frac{\sigma_0}{E_m} e^{i\phi} \tag{24}$$

$$\varepsilon_{Cm} = \frac{\sigma_0 e^{i\omega t}}{i\omega C_m e^{i(\omega t - \phi)}} = \frac{\sigma_0}{i\omega C_m} e^{i\phi} \tag{25}$$

$$\sum_{i=1}^{m} \varepsilon_i = \frac{\sigma_0 e^{i\omega t}}{E_i e^{i(\omega t - \phi)} + i\omega C_i \varepsilon_i e^{i(\omega t - \phi)}} = \frac{\sigma_0}{E_i + i\omega C_i} e^{i\phi} \tag{26}$$

The complex modulus can be determined by substituting the equations 24-26 into the expression 23. Taking its reciprocal value, it is possible to calculate the complex compliance (D^*). Similarly, it is composed by a real ($D^{'}$) and an imaginary ($D^{''}$) parts and assumes the value of equation 27.

$$D^* = D^{'} + iD^{''} = \frac{1}{E_m} + \frac{1}{i\omega C_m} + \frac{1}{E_i + i\omega C_i} \tag{27}$$

Therefore, the real and imaginary parts of the expression 27 take the following equations.

$$D^{'} = \frac{1}{E_m} + \sum_{i=1}^{m} \frac{E_i}{{E_i}^2 + \omega^2 {C_i}^2} \tag{28}$$

$$D^{''} = \frac{1}{\omega C_m} + \sum_{i=1}^{m} \frac{\omega C_i}{{E_i}^2 + \omega^2 {C_i}^2} \tag{29}$$

Finally, based on the values of the real and imaginary parts of the complex compliance, it is possible to determine the expressions to fit the laboratory values of dynamic modulus and phase angle according to the following relationships.

$$|E^*| = \frac{1}{\sqrt{D'^2 + D''^2}} \tag{30}$$

$$E^{'} = \frac{D^{'}}{D'^2 + D''^2} \tag{31}$$

$$E^{''} = \frac{D^{''}}{D'^2 + D''^2} \tag{32}$$

$$\phi = \tan^{-1}\left(\frac{D^{''}}{D^{'}}\right) \tag{33}$$

The fitting process is based on the minimization function of the sum of square errors of the predicted values of the real and imaginary parts of the dynamic modulus and the values obtained in laboratory described as:

$$F = \sum_{i=1}^{n} \left[\left(\frac{E_i^{'}}{E_i^{'0}} - 1 \right)^2 + \left(\frac{E_i^{''}}{E_i^{''0}} - 1 \right)^2 \right] \tag{34}$$

where $E_i^{'}$ and $E_i^{''}$ are the predicted values of the storage and loss modulus at the ith frequency, $E_i^{'0}$ and $E_i^{''0}$ are laboratory values of the storage and loss modulus at the ith frequency and n is the number of frequency points.

The parameters of the generalized Kelvin model were obtained by fitting the dynamic modulus and phase angle through equations 28 to 34 for loading frequencies of 10, 5, 2, 1 and 0.10 Hz, taking as reference the laboratory measurements of the viscoelastic properties of the asphalt mastics in [14], where prismatic mastic samples (80 × 50 × 50 mm) were analysed under uniaxial tensile-compressive cyclic tests at 5 °C. The number of chains associated with the model was investigated. As expected, increasing the number of Kelvin units resulted in a reduction of the fitting error. Therefore, the minimum error was obtained for a 5-element model structure. The calibrated macroscopic constants of the generalized Kelvin model are presented in Table 1.

Table 1: Calibrated parameters of the generalized Kelvin model

E_m [MPa]	C_m [MPa·s^{-1}]	E_k [MPa]	C_k [MPa·s^{-1}]
9.871×10^5	1.331×10^8	5.850×10^6	5.850×10^4
		2.486×10^6	2.486×10^5
		1.436×10^6	1.436×10^6
		4.586×10^5	4.586×10^6
		1.354×10^5	1.354×10^7

Using the calibrated parameters of the generalized Kelvin model, the fitted dynamic modulus and phase angle were compared to the experimental test results. Also, the Burger's model was fitted to the experimental data in order to compare the results with the calibrated GK model. A good agreement between the fitted and lab-based data was obtained for both dynamic modulus and phase angle with the use of the generalized Kelvin model. The calculated error using equation 26 was 0.050, a better fitting result compared to the Burger's model, with an error of 1.86.

6 INPUT PARAMETERS OF DEM MODEL

An initial guess for the parameters of the generalized Kelvin contact model for asphalt mastics is defined by converting the macroscopic properties obtained in the fitting process into contact parameters using the following set of equations:

$$\kappa_\psi^n = \frac{E_\psi A}{L}\delta \tag{35}$$

$$\eta_\psi^n = \frac{C_\psi A}{L}\delta \tag{36}$$

where L is the sum of two neighbouring particles' radii, A is the cross–sectional area of the contacting spheres, δ is a coefficient of adjustment between macroscopic properties of the asphalt mastic and DEM simulations and ψ assumes i for the Kelvin chains and m for the spring and dashpot of the Maxwell unit. The parameters for the shear direction are determined by the product of the parameters for the normal direction by α parameter, which represents the relationship between the normal and shear directions.

7 DEM SIMULATION AND MODEL VALIDATION

Numerical simulations were performed with three-dimensional mastic samples, with the height of 80 mm and length and width of 50 mm to validate the DEM model. For this purpose, two particle assemblies were generated with different number of entities. The assembly M_1 were generated with 341 discrete particles with diameters varying from 6 to 12 mm and 1825 contacts among the particles, while a more refined particle assembly M_2 were generated with 2726 discrete elements with diameters ranging from 3 to 6 mm and 14334 contacts along the sample. Figure 3 illustrates the two generated asphalt mastics.

Compressive dynamic loadings were imposed to the upper plate in the vertical direction with a strain control mechanism of 1×10^{-4} m/m, while the bottom plate remained fixed

(a) Mastic M_1 (b) Mastic M_2

Figure 3: Generated particle assemblies of mastic

in all directions. The applied loading frequencies were 10, 5, 2, 1 and 0.1 Hz. Based on the applied strain and stress monitored response of the asphalt mastic, the dynamic modulus (E^*) and phase angle (ϕ) were determined according to equations 37 and 38.

$$E^* = \frac{\sigma_{max} - \sigma_{min}}{\varepsilon_{max} - \varepsilon_{min}} \tag{37}$$

$$\phi = \frac{\Delta t}{T} \times 360 \tag{38}$$

where σ_{max}, σ_{min}, ε_{max} and ε_{min} correspond to the maximum and minimum stress responses and the maximum and minimum applied strain values. Moreover, Δt is referred to the time lag between two adjacent peak stress and strain and T is the loading period.

The parameters of the discrete element GK contact model composed by 5 Kelvin units were determined by solving the equations 35 and 36 for the normal and shear directions. A good agreement with the experimental analysis was achieved adopting values of $\alpha = 0.30$ for both mastic specimens, M_1 and M_2. Moreover, a $\delta = 1.44$ was adopted for mastic M_1 and a $\delta = 1.63$ for the particle sample M_2 were determined. The predicted values for dynamic modulus and phase for both mastic assemblies were compared to the experimental data and the results obtained with the Burger's model, as shown in Figures 4 and 5.

Numerical simulations showed a better correlation between the numerical results obtained with the GK contact model and the experimental data when compared with the agreement obtained with the Burger's contact model for both asphalt mastics. For the case of the mastic M_1, the average error for dynamic modulus and phase angle were 5.77% and 10.79%, respectively. In addition, higher values of the average errors using the Burger's contact model were obtained, where the average error for dynamic modulus was 9.67%, while 11.65% for phase angle. A similar behaviour was verified for the case of the particle assembly M_2 between the two contact models. However, the average error using the GK model was lower compared to the results obtained for mastic sample M_1, where the average errors were 4.63% for E^* and 9.40% for ϕ.

In order to investigate the influence of the α and δ coefficients on the numerical results, a parametric study was conducted with the asphalt mastic M_1 to analyse the effect on the

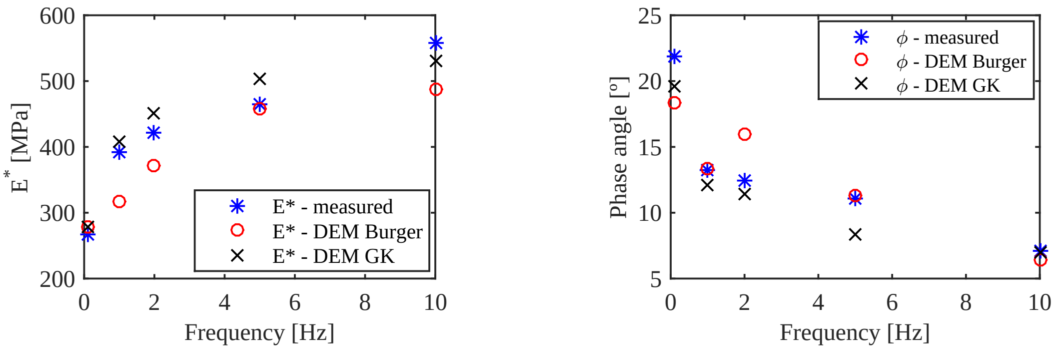

(a) Dynamic modulus (b) Phase angle

Figure 4: Comparison of the predicted and measured dynamic behaviour between the Burger's model and the generalized Kelvin model for mastic M_1

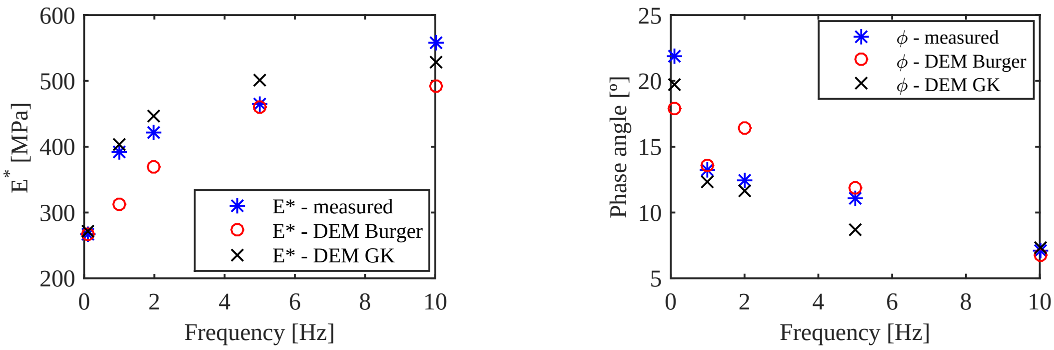

(a) Dynamic modulus (b) Phase angle

Figure 5: Comparison of the predicted and measured dynamic behaviour between the Burger's model and the generalized Kelvin model for mastic M_2

predicted dynamic response. As shown in Figure 6, the δ and α factors had no significant influence on the predicted phase angle. On the contrary, higher values of δ resulted in higher values of E^* in the analysis for directly influencing the normal and shear contact parameters. The α effect in dynamic modulus is less significant than the δ effect. The α should be calibrated in order to obtain the desired macroscopic Poisson's ratio and then the δ should be calibrated in order to obtain a good agreement with the known experimental dynamic modulus.

8 CONCLUSIONS

- A new contact model using the discrete element method approach was developed based on the macroscopic material properties in cyclic loading conditions. A good agreement with the laboratory measurements was achieved in the analysis of the viscoelastic behaviour of the mastic particle samples.

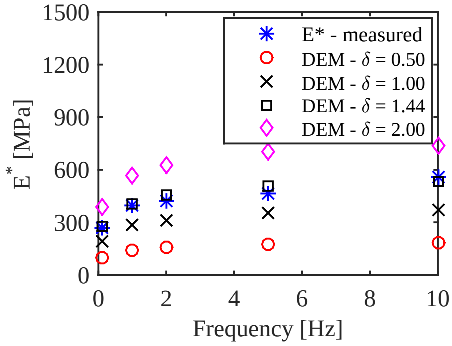

(a) Effect of δ on dynamic modulus

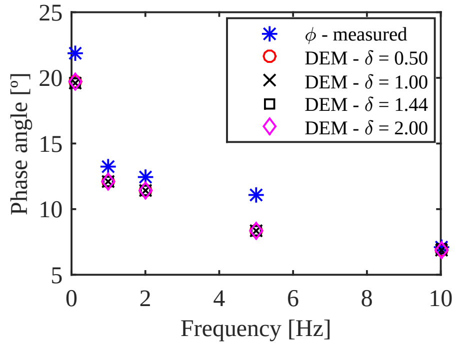

(b) Effect of δ on phase angle

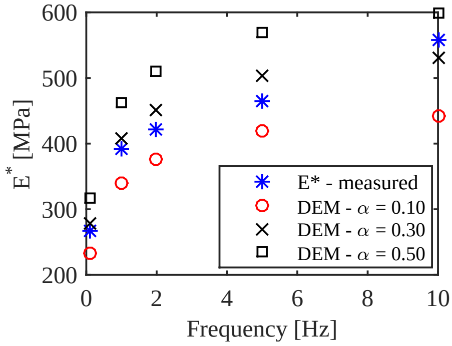

(c) Effect of α on dynamic modulus

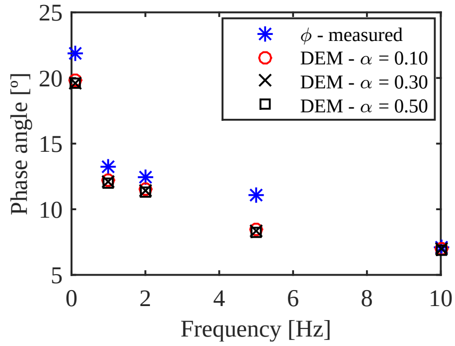

(d) Effect of α on phase angle

Figure 6: Analysis of the influence of the δ and α parameters on the dynamic modulus and phase angle response

- The developed contact model presented a better response of the dynamic modulus and phase angle of asphalt mastic compared to the Burger's model for both mastic specimens. Lower errors for both mastics, specially for mastic M_2 were obtained using the GK model.

- The methodology to determine the contact parameters of the GK model was derived. A calibration procedure was presented to convert the macroscale properties into contact parameters. With the use of stress-strain relationships and a coefficient of adjustment, the contact parameters were properly calibrated in the normal and shear directions.

- The δ parameter presented a high effect on the behaviour of the dynamic modulus as it affects the the normal and shear directions. The α parameter should be previously calibrated in order to match the macroscopic Poisson's ratio.

REFERENCES

[1] Abbas, A., Masad, E., Papagiannakis, T., and Harman, T., 2007. Micromechanical modeling of the viscoelastic behavior of asphalt mixtures using the discrete element

method. *International Journal of Geomechanics*, 7(2), 131–139.

[2] Cundall, P. A., and Strack, O. D. L., 1979. A discrete numerical model for granular assemblies. *Geotechnique*, 47–65.

[3] Buttlar, W. G. and You, Z., 2001. Discrete Element Modeling of Asphalt Concrete: Microfabric Approach. *Transportation Research Record: Journal of the Transportation Research Board*, 1757(1), 111–118.

[4] Cundall, P. A., 1971. A computer model for simulating progressive large scale movements in blocky rock systems. *Proceedings of the Symposium of International Society of Rock Mechanics*, 2(8), 129–136.

[5] Rothenburg, L., Bogobowicz, A., Haas, R., Jung, F. W., Kennepohl, G., 1992. Micromechanical modelling of asphalt concrete in connection with pavement rutting problems. *Proceedings of the 7th International Conference on Asphalt Pavements.*

[6] Chang, K.G. and Meegoda, J.N., 1997. Micromechanical Simulation of Hot Mix Asphalt. *Journal of Engineering Mechanics*, 123(5), 495–503.

[7] You, Z. and Buttlar, W. G., 2006. Micromechanical Modeling Approach to Predict Compressive Dynamic Moduli of Asphalt Mixtures Using the Distinct Element Method. *Transportation Research Record*, 1970(1), 72–83.

[8] Abbas, A., Masad, E., Papagiannakis, T., and Shenoy, A., 2005. Modelling asphalt mastic stiffness using discrete element analysis and micromechanics-based models. *International Journal of Pavement Engineering*, 137–146.

[9] Liu, Y., Dai, Q. and You, Z., 2009. Viscoelastic Model for Discrete Element Simulation of Asphalt Mixtures. *Journal of Engineering Mechanics*, 135(4), 324–333.

[10] Feng, H., Pettinari, M. and Stang, H., 2015. Study of normal and shear material properties for viscoelastic model of asphalt mixture by discrete element method. *Construction and Building Materials*, 98, 366–375.

[11] Liu, Y. and You, Z., 2011. Accelerated Discrete-Element Modeling of Asphalt-Based Materials with the Frequency-Temperature Superposition Principle. *Journal of Engineering Mechanics*, 137(5), 355–365.

[12] Ren, J. and Sun, L., 2016. Generalized Maxwell Viscoelastic Contact Model-Based Discrete Element Method for Characterizing Low-Temperature Properties of Asphalt Concrete. *Journal of Materials in Civil Engineering*, 28(2).

[13] ITASCA, 2008. Particle Flow Code in Three Dimensions, Theory and Background. *Itasca Consulting Group Inc.*

[14] Silva, H., 2005. Caracterização do Mastique Betuminoso e da Ligação Agregado-Mastique. Thesis (PhD). *Universidade do Minho.*